In Vivo Assessment of Printed Microvasculature in a Bilayer Skin Graft to Treat Full-Thickness Wounds

Maria Yanez, PhD,[1] Julio Rincon, MS,[1] Aracely Dones, BS,[2] Carmelo De Maria, PhD,[3] Raoul Gonzales, DVM, PhD, DACVPM,[2] and Thomas Boland, PhD[1]

[1]Department of Metallurgical and Materials Engineering, The University of Texas at El Paso, El Paso, Texas.
[2]Veterimnary Services, The University of Texas at El Paso, El Paso, Texas.
[3]Interdepartmental Research Center ''E. Piaggio,'' University of Pisa, Pisa, Italy.

Abstract:

Chronic wounds such as diabetic foot ulcers and venous leg ulcers are common problems in people suffering from type 2 diabetes. These can cause pain, and nerve damage, eventually leading to foot or leg amputation. These types of wounds are very difficult to treat and sometimes take months or even years to heal because of many possible complications during the process. Allogeneic skin grafting has been used to improve wound healing, but the majority of grafts do not survive several days after being implanted. We have been studying the behavior of fibroblasts and keratinocytes in engineered capillary-like endothelial networks. A dermo-epidermal graft has been implanted in an athymic nude mouse model to assess the integration with the host tissue as well as the wound healing process. To build these networks into a skin graft, a modified inkjet printer was used, which allowed the deposit of human microvascular endothelial cells. Neonatal human dermal fibroblast cells and neonatal human epidermal keratinocytes were manually mixed in the collagen matrix while endothelial cells printed. A full-thickness wound was created at the top of the back of athymic nude mice and the area was covered by the bilayered graft. Mice of the different groups were followed until completion of the specified experimental time line, at which time the animals were humanely euthanized and tissue samples were collected. Wound contraction improved by up to 10% when compared with the control groups. Histological analysis showed the neoskin having similar appearance to the normal skin. Both layers, dermis and epidermis, were present with thicknesses resembling normal skin. Immunohistochemistry analysis showed favorable results proving survival of the implanted cells, and confocal images showed the human cells' location in the samples that were collocated with the bilayer printed skin graft.

Introduction:

Chronic non healing wounds are becoming more frequent, especially in diabetic foot ulcers, which is estimated to affect around 10–15% of patients with chronic uncontrolled diabetes by 2025.[1] This will potentially require more treatments for patients with peripheral neuropathy and peripheral vascular disease, allowing the healing of chronic ulcers,[2] to avoid lower-extremity amputation.[3] Patients with diabetic foot ulcers have impaired wound healing due to a lower production of growth factors and migration of the epidermis to the wound, thereby blocking blood vessel formation, inadequate cell migration to the wound site,[4] prolonged hypoxia,[5] and chronic inflammation.[4]

One class of devices that has been shown to be somewhat effective in producing better healing of chronic wounds is tissue-engineered skin substitutes (ESS).[6] The concept typically involves a support scaffold or matrix[7] with which cells may be combined at the outset or may populate the scaffold after implantation. Although these types of ESS have been explored for over 35 years,[8] most of the available grafts today are allogeneic products and lack the vasculature needed to keep the cells alive. Thus, most, if not all, of these products require multiple applications for chronic wound treatments.

Recently, bioprinted capillaries have been built and characterized in our laboratory. It has been shown that cells such as primary keratinocytes, fibroblasts, and endothelial cells can be printed with inkjet devices onto gels with high viability rates of above 90%.[9] Furthermore, high-density cell patterns can be generated with this technique. This is possible because a new bioprinting system has been de- signed to precisely seed cells in a scaffold with minor cell damage.[10] In this study, we tested the integration of a printed vasculature imbedded into a bilayered skin graft with host tissue in a nude mouse model. Nude mice are highly utilized in wound healing research because hair re- growth does not hide the wound healing process.[9] Most of the studies that have been done in nude mice create a full- thickness wound in the dorsum of the mouse. Mouse wound healing shows wound contraction close to 90%, which is significantly different in human wound healing.[11] However, the athymic nude mouse model provided the opportunity to demonstrate the scaffolding abilities of engineered skin grafts and to measure how much the graft's architecture compares to normal skin architecture after healing is completed. In addition, the athymic nude mouse model allows the study of the integration of the engineered tissue without interference from immune rejection. Wound contraction is part of the normal healing process, but if the contraction is too large, it can cause malfunction and cosmetic

problems in the wound area of the patient.[4,5] The objective of this study was to characterize the *in vivo* response to the engineered skin grafts compared to no graft and the commercially available Apligraf®. Apligraf attempts to mimic the structure of the skin by providing with two layers that are equivalent to the epidermis and dermis, containing keratinocytes and fibroblast obtained from neonatal foreskin.[12] The bottom layer is composed of bovine collagen type I mixed with fibroblasts. At the top of the collagen is a layer with keratinocytes. Apligraf is FDA approved for diabetic foot ulcer and venous leg ulcer treatment. It is supplied as a circular disk (7.5 cm in diameter and 1 mm thick).[13] The cells in this graft do not survive *in vivo,* so it is considered a temporal dressing.

Materials and Methods

Scaffold fabrication

Collagen type I, bovine cell culture grade (5 mg/mL) was from Gibco Invitrogen, fibrinogen from bovine plasma, thrombin from bovine plasma, phosphate buffered saline (PBS), 10x Dulbecco's modified Eagle's medium (DMEM), 1N NaOH were obtained from Sigma. Collagen gels were prepared by mixing the appropriate amount of 10x DMEM, milli-Q water, 1N NaOH, and collagen type I to reach a final concentration of 3.2 mg/mL, keeping all solutions in ice until used. The solutions were separated in two different sterile falcon 15 mL centrifuge tubes and kept on ice for further use.

Neonatal human dermal fibroblast (NHDF), human der- mal microvascular endothelial cells (HMVECs), and neo- natal human epidermal keratinocytes (NHEK) were purchased from Lonza, maintained and subcultured according to the manufacturer's protocol. NHDF were maintained on DMEM supplemented with 10% fetal bovine serum (FBS) and 1% antibiotic/antimycotic solution, HMVEC on endothelial growth medium (EGM) supplemented with hydrocortisone, human epidermal growth factor (hEGF), FBS, vas- cular endothelial growth factor, human fibroblast growth factor-basic, human recombinant analog of insulin-like growth factor-I with the substitution of Arg for Glu at position 3 (R3-IGF-1), ascorbic acid, heparin, and gentamicin/ amphotericin-B. NHEK were maintained with keratinocytes growth media supplemented with bovine pituitary extract, hEGF, insulin, hydrocortisone, transferrin, epinephrine, and gentamicin/amphotericin-B. Cells were incubated at 37°C in a 5% CO_2 environment.

NHDFs were trypsinized, counted, and added to the collagen solution previously separated in a falcon 15 mL centrifuge tube, obtaining a final concentration of 2×10^6 cell/mL. Five hundred microliters of collagen- NHDF solution was pipetted on a glass slide and then placed in the incubator at 37°C in a 5% CO_2

environment for 30 min. Gelation was assessed by touching the collagen gel with a sterile 1 mL pipette tip. Thrombin was dissolved in 0.08 M of $CaCl_2$-PBS solution with a concentration of 40 NIH U/mL. Fibrinogen was dissolved in milli-Q water with a concentration of 60 mg/mL as described before.[14] HMVEC cells were trypsinized, counted, and mixed with thrombin solution to obtain a final con- centration of $2x10^6$ cell/mL.

To fabricate the bilayered structure shown in Figure 1A, the collagen-NHDF gel was placed onto the deposition plate of a cell printer developed in our laboratory.[15] Two hundred fifty microliters of thrombin-HMVEC solution were placed inside a modified printer cartridge and 200 mL of the fibrinogen solution were pipetted onto the collagen-NHDF gel. Then, the HUVEC-thrombin solution was printed. The samples were then incubated for 10–20 min to allow the fibrin to form. To finish the bilayer structure, the NHEK cells were trypsinized, counted, and added to the second collagen solution with a final concentration of $2x10^6$ cell/mL. Two hundred microliters of this solution were pipetted on top of the fibrin gel and the entire construct was incubated again for 30 min. The dimensions of the printed skin grafts are 2.5 · 5 cm with a thickness of 1.2 mm. The samples were placed in 6 cm Petri dishes with 4 mL of EGM growth media, and incubated at 37°C in a 5% of CO_2 environment for 24 h before being grafted. There was some contraction of the gel to yield final dimensions of 2 cm x 4.5 cm x 1 mm. These dimensions were chosen to be as close to the Apligraf as possible, with the exception of the printed endothelial cells. The entire construct is referred to as printed skin graft, keeping in mind that only the vascular layer was printed (Fig. 1B).

For *in vivo* experiments the endothelial cells were stained with PKH26 red fluorescence cell membrane labeling dye before the printing process to assess the cells and micro- channel formation over time. The labeling protocol of the manufacturer was followed. Briefly, cells were suspended in diluent C and PKH26 was diluted in diluent C at 4 mM. The PKH26 solution was mixed with the cell suspension and kept in the dark for 5 min to allow the dye to bind to the cell membrane, swirling gently to assure the dye distribution. The reaction was then stopped by adding an equal amount of serum-supplemented media.
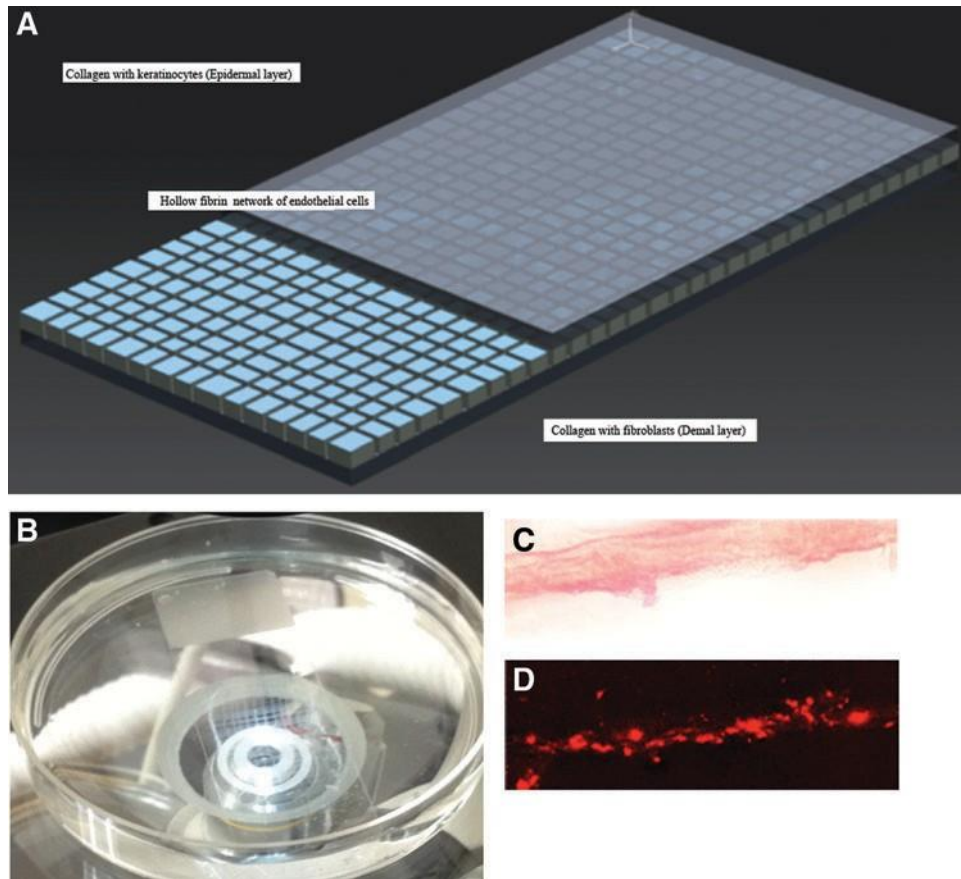
FIG. 1. (A) Schematic representation of the print- able skin graft. The top and bottom layers are made of collagen with dispersed keratinocytes (top) and fibro- blasts (bottom). The middle layer is a fibrin gel with endothelial cells. (B) Photo- graph of the printed patterns. Representative bright- field of the gel printed pat- tern. (D) Confocal image of the patterns visualizing the PKH26 stained HMVECs. HMVECs, human dermal microvascular endothelial cells. Color images available online at www.liebertpub.com/tea

Animal surgical procedure

Animal protocol was approved by the Institutional Animal Care and Use Committee (IACUC) at The University of Texas at El Paso (UTEP). Sixty male, athymic nude mice (homozygous nude $Foxn1^{nu}/Foxn1^{nu}$; strain name: J:NU; stock number: 007850) were purchased from The Jackson Laboratory and housed in the animal care facility located in the Bioscience Research Building on UTEP. The animals were housed under barrier conditions. Sanitization and strict aseptic technique was followed during the surgical procedure and postoperative animal care. On the day of the surgery, the mice were anesthetized with intraperitoneal injection using ketamine (50 mg/kg)/xylazine (5–8 mg/kg) and maintained (1–2%) on isoflurane anesthesia using a portable anesthesia machine (EZ-Anesthesia Classic Lab Research Anesthesia System). The animals were placed on a warmed heating platform to provide additional warming during the surgical procedure while their body temperature was monitored using a rectal probe. The graft area was surgically scrubbed using Betadine Surgical Scrub followed by 70% ethanol, repeated three times. Then, 0.5 mL of 25%

marcaine was injected along the incision site for aditional analgesia, and pain relief.

The animals were covered with a clear sterile surgical incise drape (3M™ Ioban™ 2 Antimicrobial Incise Drape), which allows the incision site to be directly viewed as the work area could have been viewed through the material. Full-thickness skin incisions, 2 mm deep, measuring 1.7 x 1.7 cm were performed using a No. 15 scalpel blade, penetrating down to the subcutaneous tissue. The skin was reflected back and removed. The wounds were 30–40% to the dorsal of each animal. Bleeding was controlled with direct pressure on the wound site using a sterile guaze pad, or by using small mosquito hemostats on any small vessel bleeding, or with a small pen electrocautery unit. Maximum blood loss allowed was no more than 10–15% of the animal's blood volume or 0.3–0.5 mL. The printed skin grafts were placed on the full-thickness wounds. The printed skin graft and Apligraf were cut according to the dimensions of the full-thickness wound. For the control group, the wound was either covered with Apligraf, or not covered by Mepitel®, a nonadherent silicone dressing to keep the moisture, protect the wound site, and keep the skin graft in place. The Mepitel was sutured using a 4-0 prolene non-absorbable suture along the edge at six different points. A sterile, fine mesh gauze impregnated with petrolatum (Xeroform®) covered the Mepitel to protect the wound site, and to maintain a moist wound environment. Xeroform was sutured on each point to secure the pad to the animal using a single 4-0 prolene nonabsorbable suture.

The animals had a postoperative sub-Q injection of 0.1–0.2 mg/kg buprenorphine, which was induced when the animals completely recovered from the surgical procedure, 20 min after surgery. Postoperative analgesia was induced with buprenorphine every 8 h (q8) for the first 2 days if the animals were in pain, then as needed for pain relief.

After the surgical procedure, the animals were placed in sterilized, individually ventilated cages with sterilized surgical bedding (diamond chip bedding; Shepard Specialty Paper Co.) and additional warming was provided during recovery. The animals were continuously monitored during the recovery period until they were any type of skin graft. The grafts were then covered by fully ambulatory and foraging with no overt signs of pain/distress.

The sutured pad was allowed to stay in place for 8–10 days to allow for full healing in the wound area, during which time the animals were monitored at a minimum of twice daily for pain/distress, self mutilation, infections and surgical pad placement, and adequate healing. The mice were monitored until completion of

the specified experimental time line, at which time the animals were humanely euthanized and tissue samples were collected. The tissue was fixed in 10% buffer formalin, and processed for histological and immunohistochemical analysis.

Wound contraction

Mice were photographed the day of the surgical procedure and at the end point; a ruler was next to the wound site to determine the right scale.[16,17] Wound area at each time point was determined using the ImageJ software.[17] The percentage of wound contraction was defined as follows:

$$\% \, wound \, contraction = \left(1 - \frac{wound \, area \, at \, the \, endpoint}{wound \, area \, at \, the \, surgery}\right) \times 100$$

Histology

The tissues harvested inlcuded the contracted skin and the regenerated skin. Tissue samples were processed using a Spin Tissue Processor (Microm STP-120; Thermo Scientific). The dehydration process was carried out by immersing tissue samples in different concentrations of ethanol (starting with 70%, 95%, 100%), then was followed by the clearing process where samples were immersed in xylene three times, and finally samples were infiltrated in paraffin. Tissue samples were embedded in paraffin and sectioned with a thickness of 6 mm using a Shandon Finesse® E/ME microtome. The tissues were sectioned to include the contracted skin and the regenerated skin in the same section. Tissue samples were stained with hematoxylin and eosin (H&E) staining. Samples were mounted with a cover glass and observed under a microscope to determine the epithelial and scar thickness.[18–20] Epithelial thickness was determined using H&E stained cross-sections at the wound margin.[19] Epidermal thickness of the neoskin was determined by measuring epidermis and dermis thickness of H&E stained cross-sections of new skin.[20]

Immunohistochemistry

Tissue sections for immunohistochemistry (IHC) were deparaffinized in xylene, and hydrated using successive concentrations of ethanol starting from 100%, 95%, 70%, 50% and finishing with distilled water. For antigen un- masking, the samples were boiled for 15 min in antigen retrieval solution consisting of 10 mM sodium citrate, 0.05% Tween 20 at pH 6.0, cooled on a bench top for 30 min, and rinsed with 1x PBS. Cells were permeabilized with 100% methanol at - 20°C for 6 min to provide access to the antibody. Tissue samples were blocked for 1 h at room temperature in 5% normal goat serum. Samples were incubated for 1 h at room temperature with mouse monoclonal Anti- Nuclei Antibody, clone 235-1 (GeneTex) in PBS (1:100).

Unbound antibody was removed by washing the samples three times with PBS 10 min each. Subsequently, samples were incubated for 1 h at room temperature with Cy™ 3- conjugated AffiniPure Donkey Anti-Mouse IgG (Jackson ImmunoResearch Laboratories) in PBS (1:500). The samples were rinsed as before, and during the final rinse, the cells were incubated with DAPI. Samples were mounted with DAKO mounting media (DAKO Corp.) and covered with a coverslip. Imaging was performed with a Nikon Eclipse Ti microscope and Nikon D-Eclipse C1 Confocal unit and Software.

Statistical analysis

Arithmetic mean and standard deviation were calculated for all quantitative data. The printed skin graft group data were compared with the control group data and Apligraf group data at the different time points using Student's *t*-test. A value of $p < 0.05$ was considered statistically significant.

Results

In vitro assessment

Figure 1C shows the printed pattern of HMVEC using the bright-field and Figure 1D are the HMVEC stained with PKH26 red fluorescence cell membrane labeling at day 6. One can clearly see that the cells are aligned in the printed pattern and are trying to connect to each other. Inkjet printing is a good technique to deposit cells in specific locations without cell damage, which allows for microvessel formation.

Macroscopic observations

Following transplantation, the printed skin grafts were initially viable, pink, and soft whereas meshed Apligraf grafts were white. Figure 2 shows the grafting procedure at different time points; surgical preparation (Fig. 2A), full- thickness wound (Fig. 2B), application of the engineered printed skin graft (Fig. 2C), application of Apligraf (Fig. 2D), application of Mepitel (Fig. 2E), and application of Xeroform (Fig. 2F). At day 7 after the surgical procedure, Apligraf appeared yellow, and by day 14 Apligraf dried out and visibly detached from the wound site (Fig. 3A), whereas the engineered skin grafts adhered to the wound tissue (Fig. 3B). No infection was observed over time in any of the groups. The mice with printed skin grafts healed by the beginning of the third week and it is estimated that full closures were achieved sometime between 14–16 days. The mice in the control group achieved closure at the end of the third week or 21 days. Finally, the mice with the Apligraf healed at the end of the fourth week or 28 days, and in 3 out of 10 cases the wound was not completely closed at the end of the fourth week, which was the latest endpoint studied.
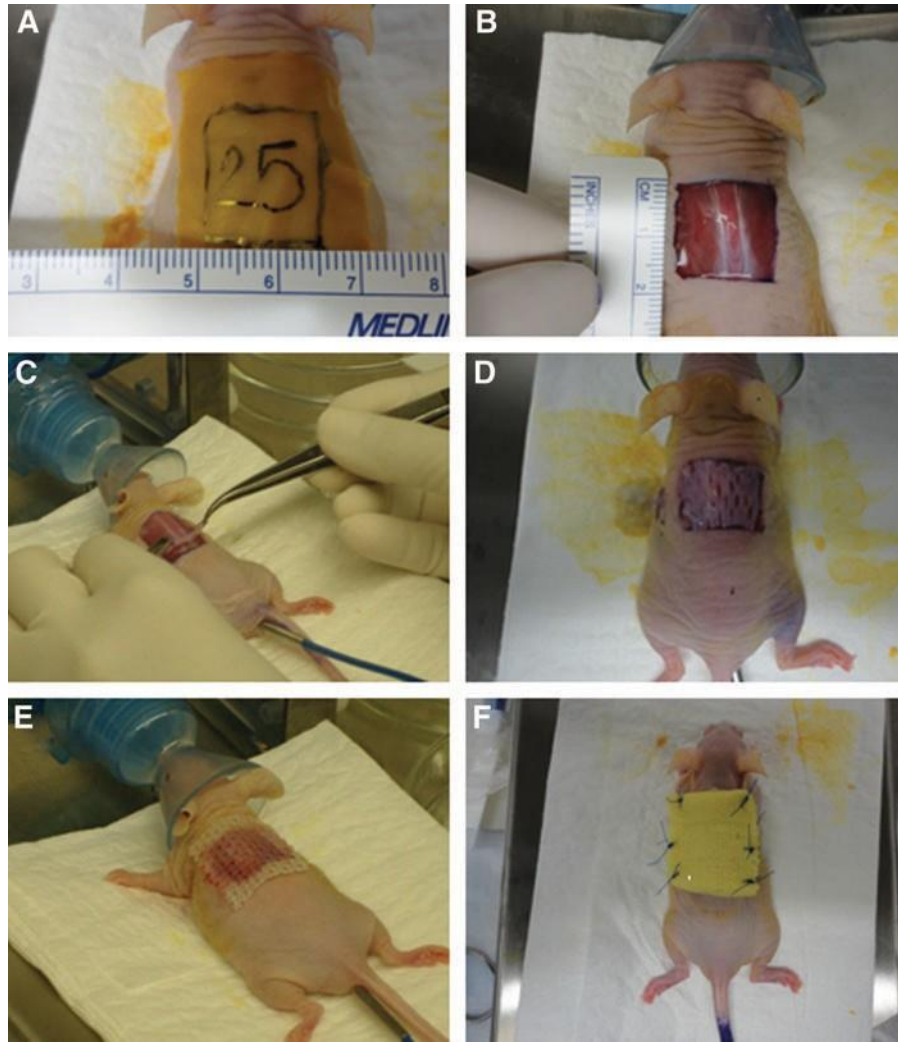
FIG. 2. Surgical procedure at different time points showing the full-thickness wound and graft procedures. (A) The area is marked with a standardized template, (B) the full-thickness wound is documented, (C) the printed skin graft is applied, (D) the Apligraf® is ap- plied, (E) the Mepitel® is sutured in six different points, and (F) the Xeroform® is applied. Color images available online at www.liebertpub.com/tea

Wound contraction

Results of the wound contraction are shown in Figure 4. The percentages of wound contraction with respect to the wound on day 0, in the group with the printed skin graft were 69% – 4%, 71% – 2.4%, 66% – 9%, 68% – 4.4%, and 62.5% – 9% at week 2, 3, 4, 5, and 6, respectively. The wound contraction slightly decreased over time. In the Apligraf graft and the control group, the wound contractions were larger than in the printed skin graft group; 17% when compared to the Apligraf group and the control group. The percentage of wound contraction in the comparative group with the commercial skin graft was 80% – 2.3%, 79% – 5% at week 4 and 6, respectively. The percentages of wound contraction for the control group were 75% – 9%, 74% – 5%, 80% – 4.5%, and 79% – 2% at week 2, 3, 4, and 6, respectively. Peak contractions were 69% for the printed skin graft group and 75% for the control group. The wound area decreased over time. There was not a significant

difference in wound contraction between the groups at week 2. However, both at week 4 and 6, the contraction was significantly lower ($p < 0.05$) for the group with printed skin when compared to either group Apligraf or control. The wound contraction for the Apligraf group did not differ significantly from the contraction in the control group at any time point.
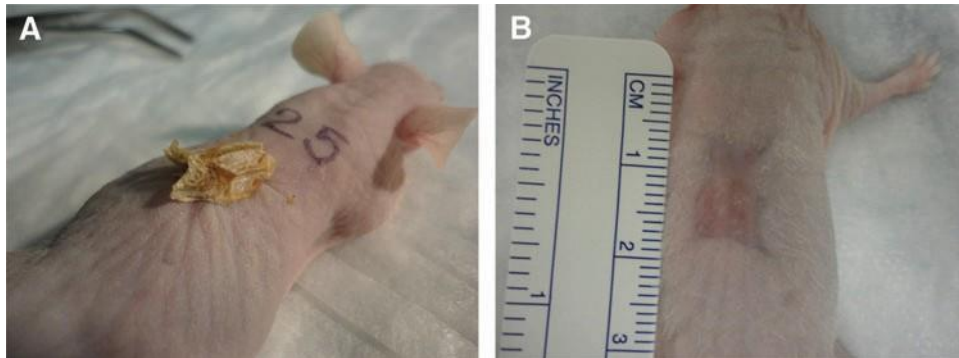

FIG. 3. Macroscopic observations of the skin grafts after 4 weeks postimplantation. (A) The Apligraf is ap- plied to the wound. (B) The regenerated skin when a printed skin graft was applied to the wound site. Color images available online at www.liebertpub.com/tea
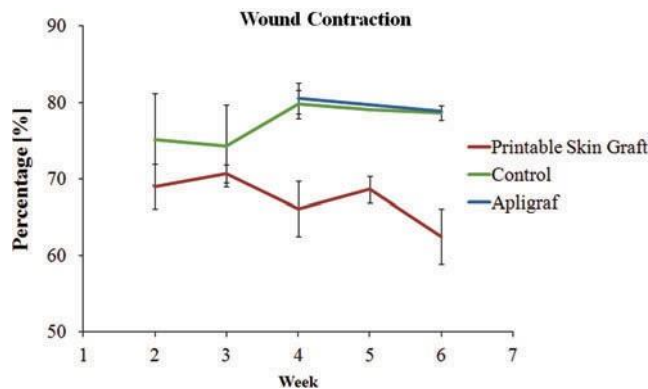

FIG. 4. The graph is showing the wound contraction in the experimental groups (printable skin graft and commercial skin graft, Apligraf), and in the control group at the end point of each group between week 2 through week 6 (n = 5). There is not a significant difference between the printable skin graft and control groups at week 2 ($p < 0.05$). However, there was found a significant difference between the groups when compared with the printable skin at week 4 and 6 ($p < 0.05$). Color images available online at www.liebertpub.com/tea

Histology

Representative H&E stained tissue sections of the different groups during animal testing is shown in Figure 5. In all groups, the epidermal and dermal layers were present, including the group treated by the Apligraf (Fig. 5A). In 2 of 15 collected tissues where the Apligraf was applied, the epidermal layer was thicker than in the other cases and showed evidence of hypergranulation probably due to an extended inflammatory response. The H&E stained sections of the untreated control group show extensive scar tissue formation (Fig. 5B). The wounds covered by the printed skin grafts presented almost the same thickness for both

dermal and epidermal layers as the normal mouse skin (Fig. 5C). The only difference is that uninjured mouse skin shows sebaceous glands (SG), some hair follicles, and hair bulbs. In addition, the sections show evidence of new blood vessel formation in the new skin when the wound bed was covered by the printed skin graft (marked by black arrows in Fig. 5D). This formation is interpreted due to printed HMVECs in the graft. To assess the proangiogenesis of the fibrin gel without any cells, a fibrin gel alone was subcutaneously implanted in the back of the mouse and no blood vessel formation was observed when the tissue sample was stained with H&E (data not shown).
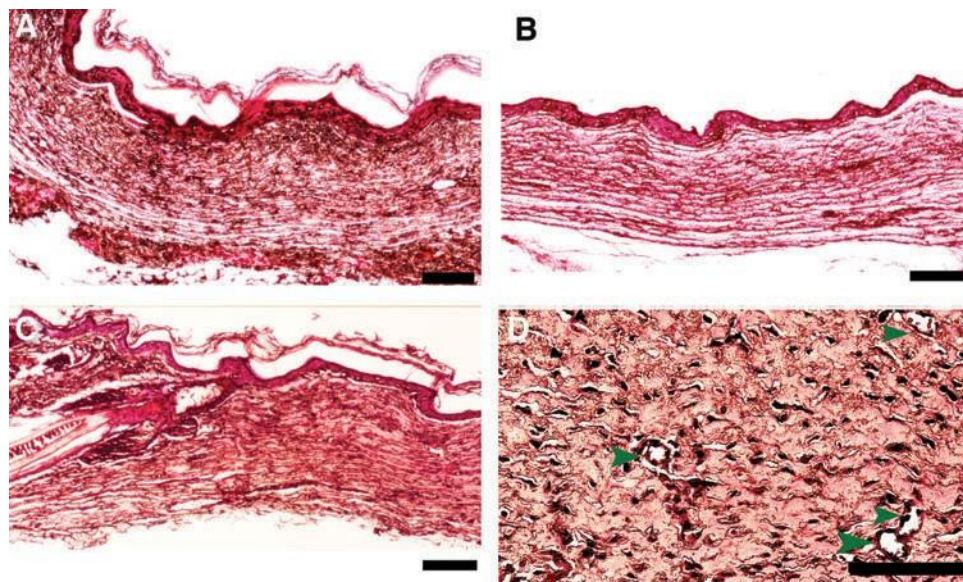

FIG. 5. Representative H&E stains of neoskin (10 · micrographs). (A) Commer- cial skin graft after 4 weeks. No grafts after 4 weeks. Printable skin graft after 4 weeks. (D) Printable skin graft after 2 weeks, *green arrow heads* indicate the small microchannels found in the new skin (this image was taken at a higher magnification). The scale bars are 100 mm. H&E, hematoxylin and eosin. Color images available online at www.liebertpub.com/tea

Epidermal and epithelial thickness

At week 6, the total epidermal thickness was 239 – 35 mm in the printed skin graft group, 289 – 190 mm in the Apligraf group, whereas 208 – 73 mm for the control group without graft. The Apligraf group has a high standard deviation because one mouse in this group had a thicker dermal layer than the other mice in this group. There is not a significant difference between the three different groups. The mean of the epithelial thickness was 29.7 – 4.2 mm for the printed skin graft group and 16.8 – 8 mm in the Apligraf group, whereas 21.5 – 7.6 mm for the control group without graft after week 6 postsurgery. The mean for the epithelial thickness in the printed skin graft group is significantly thicker than in the commercial skin graft and the control group (p = 0.05). This data implies that ⁓90% of the epi- dermal layer regenerated in the printed skin graft, whereas 50% regenerated in the Apligraf-treated group, and 60% regenerated in the untreated control group.

In addition, histological analysis revealed that all major features of the healed skin is accurately recapitulated in mice when a printed skin graft is implanted, and depicted the remodeled tissue which contains both dermal and epidermal layers.

Immunohistochemistry

Figure 6 shows the IHC staining for the mouse skin with a printed skin graft at week 2 (Fig. 6A, B), and for the Apligraf group at week 4 (Fig. 6C, D). Figure 6A shows all the nuclei of the cells (human and mouse cells) in the mouse tissue (blue), and the presence of microvessels can be ob- served. These must have formed after the transplantation of the printed skin graft (white arrow head) when the vessels are stained positive for human genes (Fig. 6B).
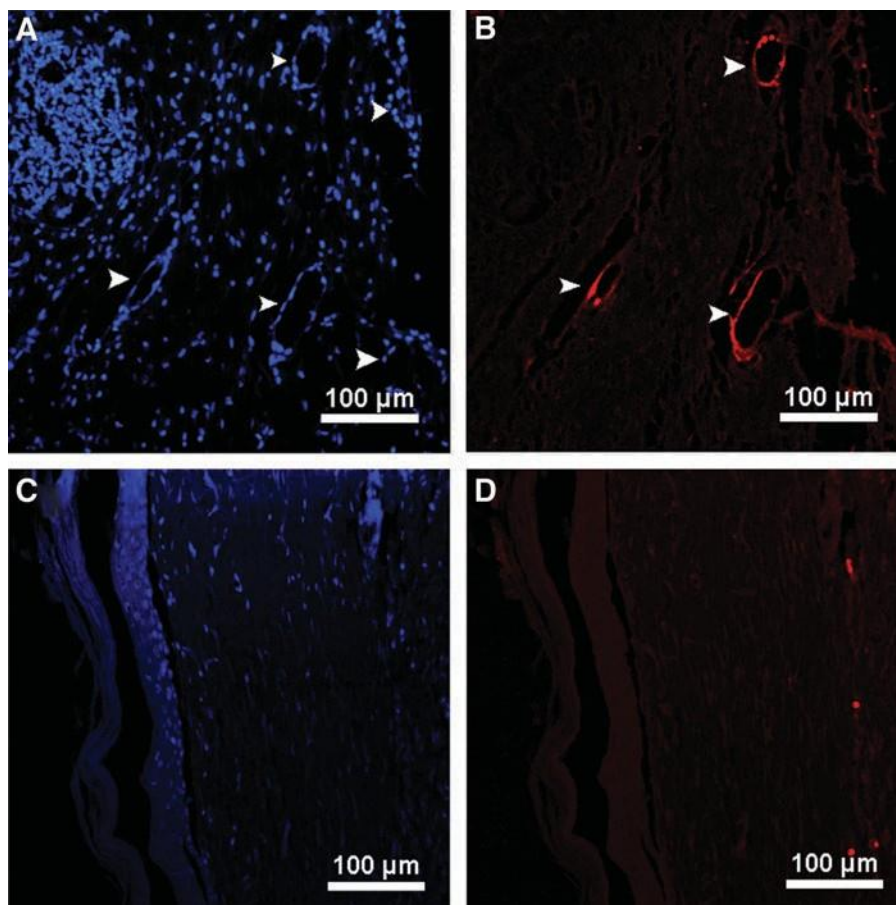

FIG. 6. Immunohistochemistry staining of neoskin after grafting on human skin equivalents. (A, B) Mouse skin with the printable skin graft at week 2. (C, D) Mouse skin with Apligraf skin graft at week 4. The tissues were stained with Anti-Nuclei Antibody, Clone 235-1, and visualized with Cy 3 conjugated AffiniPure Donkey Anti-Mouse IgG (H + L) (red). (A, C) DAPI staining for the nuclei of the cells in the tissue section (mouse and human cells), the *white arrow heads* show the presence of the microvessels in the mouse tissue. (B, D) The stained nuclei of the human cells present in the mouse skin (*bright red*). Color images available online at www.liebertpub.com/tea

This further confirmed that part of the graft integrated to the mouse skin and helped to form new microvessels and implies that the neoskin was regenerated with the human cells administered through the printed skin

graft. As these sections are stemming from an area near the mouse–graft interface, the presence of human cells in the mouse tissue suggests that the contracted old mouse skin contains immigrated human blood vessels. Thus, we think that the human endothelial cells were recruited from the graft to form neovessels in the contracted dermis potentially resulting in graft–host anastomoses. Figure 6D shows the IHC staining for the mouse skin after grafting of the Apligraf at week 4. Although there may be some evidence of human cells in the neoskin of the mice after Apligraf grafting, as judged by the bright red nucleus at the top and at the bottom of the image, there is clearly less human cell integration in the host tissue when compared to the printed bilayer grafts. This is further sup- ported by the reported short-term life of Apligraf, or the death of the majority of the cells within the graft, which may be due to the dehydration of the graft (Fig. 3A).

Although the fibrin gel described above does not mimic the normal human extracellular matrix of skin, it is a temporary blood clotting matrix that forms in wounds that eventually will be replaced by other extracellular matrix proteins as the wound heals. We would test this hypothesis by quantifying the wound healing and comparing it to the healing of a commercially available skin construct. From the results obtained in this study, it is evident that the matrix was replaced by a matrix that approximates uninjured mouse skin within 2–3 weeks postimplantation. The replaced tissue resembled native tissue in many respects, such as thickness of both epidermal and dermal layers, structure of both layers are very similar to uninjured mouse skin and cell content, except the lack of glands and hair follicles. The epidermal layer showed normal keratin in the stratum corneum. Keratinocytes were found in the epidermal layer with the sim- ilar structure as the keratinocytes observed in the uninjured mouse skin. The dermal layer showed evidence of blood vessels. It is evident from the H&E staining that the re- modeled tissue is more related to uninjured mouse skin than scar tissue when the printed graft was applied.

Figure 7A shows the H&E staining of the healed tissue of control animals with neither Apligraf nor printed grafts. In these animals, we observed mainly mature scar tissue marked with black arrow in the figure. In addition, we observed very few residual fibroblast cells marked by green arrows. Figure 7B shows uninjured mouse skin stained with H&E. As expected, we observed the epidermis and dermis, including SG and some vessels marked by red arrows.
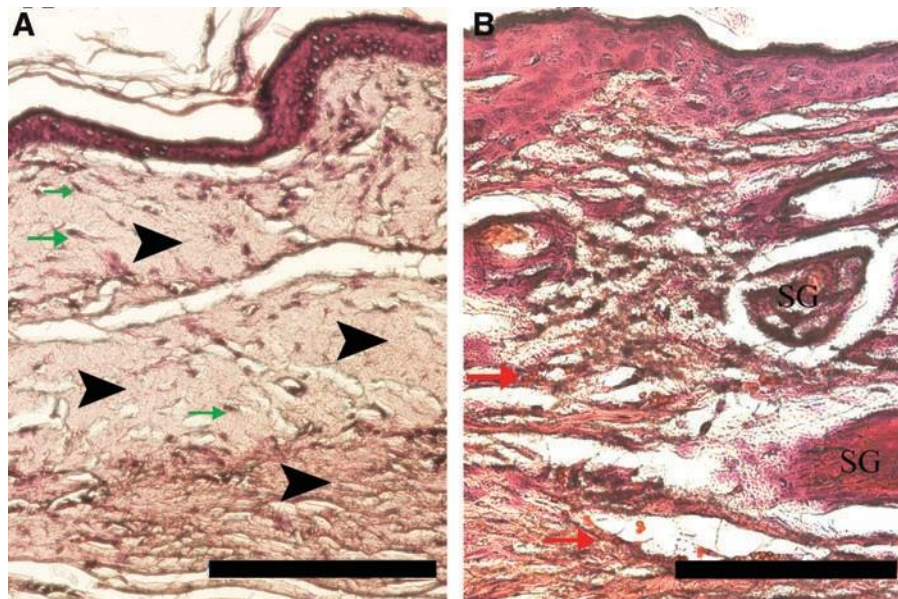
FIG. 7. H&E staining for scar tissue (A). Black arrow heads in-dicate mature scar tissue, green arrows mark residual fibroblasts. (B) H&E stain of uninjured mouse skin. Red arrows mark some vessels; the presence of sebaceous glands is denoted SG. The scale bar is 100 mm. SG, sebaceous glands. Color images available online at www.liebertpub.com/tea

Discussion

The main objective of this research was to evaluate the capability of the printed skin graft as a dermo-epidermal skin graft after a full-thickness wound was created on the dorsum of an athymic nude mouse. The transplantation of the printed skin grafts in athymic nude mouse in the dif-ferent groups, healed at different rates of time. Previous studies have shown that composite epidermal skin grafts healed 1 week faster than control mice in a comparable experimental setup,[21] corroborating with our results. Clinical data showed that Apligraf may degrade partially or completely after the initial application and in 3–5 days may have an appearance of yellow gelatin.[22] Apligraf is also known to pull off easily during dressing changes.[22] The printed skin graft and Apligraf have the main layers of the skin, epidermis and dermis, supplemented with human cells. Both Apligraf and the printed skin graft have comparable thickness (1 mm). Both grafts are cut to fill the full thickness wound. The only important difference between both grafts is the additional printed fibrin layer with human endothelial cells in the printed skin graft. Apligraf contains dermal fibroblast, seeded at 30,000 cells/mL, which are cultured for 6 days, then the keratinocytes are seeded at 10^5 cells/mL, and the construct is cultured for 10 days at the air–water interface. In contrast, the concentrations of fibroblast and keratinocytes in the printed grafts are higher (2×10^6 cell/mL), but there is only a 24 h-submersed culture before implantation. Still, the number of cells at the time of implantation is comparable between the two grafts as the cells in the Apligraf will proliferate during the 2 week culture.

Wound contraction is part of the healing process in which the edge of the wound is closing to the center.[23] Wound contraction depends of the species, age, wound dimension, and so many other parameters.[23] Usually, in adult humans the wound contraction is between 20–40%, whereas in other mammalian it is between 80–90% (rats and mice).[23,24] Excessive wound contraction leads to a clinical morbidity due to joint contracture, malfunction, and cosmetic prob- lems.[23,25] In this study, we found the wound contraction is improved when the printed skin graft is applied in a full-thickness wound in athymic nude mouse model. We believe that may be an improvement in human chronic ulcers if the printed skin graft is applied; however, studies need to be performed to know the behavior of the printed skin graft when applied in humans with chronic wounds. Previous studies reported that when a graft is applied on a wound bed, the wound contraction and scarring might be reduced.[26] The wound contraction was improved by 17% with the printed skin graft when compared with the other two groups (Apligraf and control). Furthermore, we found that the wound con- traction decreased over time. This could be related to the tissue remodeling into normal tissue.[27] In studies that used human fibroblast and human keratinocytes in a collagen– glycosaminoglycan sponge, the contraction was 64% after 6 weeks postgraft.[28]

In the control group the percentage of the wound con- traction slightly increased over time, as did those in the commercial skin graft. Again, this is expected and was found in previous research, which also documented a peak of wound contraction between the second and third week[28,29] and is attributed to the scar formation, which[30] we documented by histology.[29] The wound contractions re- ported in this study are consistent with the previous studies done by Kalyanaraman & Boyce, who fabricated an ESS using a Kerator bioreactor.[28] In those studies, a collagen–glycosaminoglycan matrix was employed with seeded human fibroblast and human keratinocytes. Other studies performed with athymic mouse model revealed that when keratinocytes and fibroblast cells are seeded onto an acellular collagen– glycosaminoglycan matrix augmented with vitamin C is implanted on a full-thickness wound, the wound contraction is 70% at week 6.[29] The histological findings revealed that the epidermal and

dermal layers are found on postoperative day 14 when a printed skin graft was applied. The application of the printed skin graft allows the formation of new microvessels. This is attributed to the endothelial cells that were seeded in the skin graft. In addition, human keratinocytes are known to secrete various angiogenic growth factors.[21] Previous work revealed that when human acellular dermis was infiltrated with HaCaT epidermal cells and supplemented with a fibrin gel and antigenic factors, it enhanced neovascularization.[30–32]

Studies performed by Kremer *et al.* revealed that when Integra® was seeded with keratinocytes and implanted on a full-thickness wound, the matrix infiltrated in the wound bed.[33] Other studies have shown that when a collagen matrix with keratinocytes and fibroblasts is implanted in a full-thickness wound, the epidermal and dermallayers are present in the neoskin.[28,29,34]

There is clearly room for improvement in existing skin grafts, and adding endothelial cells to a network is a step in this direction. There is some evidence that the addition of endothelial vessel networks will achieve viable integration. One possibility of how those vessels will integrate with neighboring vasculature or support viability *in vivo* is due to the same mechanism that is involved in full-thickness grafts or cadaver grafts integration. These processes are not completely understood and depend on the type of graft, the wound bed preparation, and nature of the inflammatory response of the host. While we have not delineated all these effects here, we did establish that the presence of endothelial networks throughout the graft can maintain the graft's life for a longer period than skin grafts lacking these networks and the endothelial cells will become integrated with the vasculature host. Whether the networks actually anastomose with host vessels or whether the endothelial cells get primarily recruited by the remodeling tissue is yet to be determined.

Conclusions

In the current study, a new printed skin graft was shown to accelerate the wound healing when it is compared with a commercially available skin wound dressing (Apligraf), and without any type of dressing. The transplantation of printed skin graft transfers part of the artificial *in vitro* cultivation to the wound area allowing the wound to heal. Wound con- traction was improved by up to 17% when compared with the other two groups. Histological analysis showed that the neoskin was closely related to the normal skin. Immuno-fluorescence studies showed the presence of human cells at the fourth week postsurgery.

Disclosure Statement

References

1. Boulton, A.J. The diabetic foot: a global view. Diabetes Metab Res Rev 16 Suppl 1, S2, 2000.
2. Gray, M., and Peirce, B. Is negative pressure wound therapy effective for the management of chronic wounds. JWound Ostomy Continence Nurs 31, 101, 2004.
3. Frykberg, R.G. Diabetic foot ulcers: pathogenesis and management. Am Fam Physician 66, 1655, 2002.
4. Blakytny, R., and Jude, E. The molecular biology of chronic wounds and delayed healing in diabetes. Diabet Med 23, 594, 2006.
5. Falanga, V. Wound healing and its impairment in the diabetic foot. Lancet 366, 1736, 2005.
6. Curran, M.P., and Plosker, G.L. Bilayered bioengineered skin substitute (Apligraf): a review of its use in the treatment of venous leg ulcers and diabetic foot ulcers. Bio- Drugs 16, 439, 2002.
7. Langer, R., and Vacanti, J.P. Tissue engineering. Science 260, 920, 1993.
8. Bello, Y.M., Falabella, A.F., and Eaglstein, W.H. Tissue-engineered skin. Current status in wound healing. Am J Clin Dermatol 2, 305, 2001.
9. Cui, X., Boland, T., D'Lima, D.D., and Lotz, M.K. Thermal inkjet printing in tissue engineering and regenerative medicine. Recent Pat Drug Deliv Formul 6, 149, 2012.
10. Cui, X., Dean, D., Ruggeri, Z.M., and Boland, T. Cell damage evaluation of thermal inkjet printed Chinese hamster ovary cells. Biotechnol Bioeng 106, 963, 2010.
11. Benavides, F., Oberyszyn, T.M., VanBuskirk, A.M., Reeve, V.E., and Kusewitt, D.F. The hairless mouse in skin re- search. J Dermatol Sci 53, 10, 2009.
12. Wilkins, L.M., Watson, S.R., Prosky, S.J., Meunier, S.F., and Parenteau, N.L. Development of a bilayered living skin construct for clinical applications. Biotechnol Bioeng 43, 747, 1994.
13. Morgan, J., and Yarmush, M. Bioengineered skin substitutes. Sci Med 4, 6, 1997.
14. Cui, X., and Boland, T. Human microvasculature fabrication using thermal inkjet printing technology. Biomaterials 30, 6221, 2009.
15. De Maria, C., Rincon, J.E., Duarte, A.A., Vozzi, G., and Boland, T. A new approach to fabricate agarose micro- structures. Polym Adv Technol 24, 895, 2013.
16. Garcia, M., Escamez, M.J., Carretero, M., Mirones, I., Martinez-Santamaria, L., Navarro, M., Jorcano, J.L., Meana, A., Del R´ıo, M., and Larcher, F. Modeling normal and pathological processes through skin tissue engineering. Mol Carcinog 46, 741, 2007.
17. Bannasch, H., Fohn, M., Unterberg, T., Knam, F., Weyand, B., and Stark, G.B. Skin tissue engineering. Clin Plast Surg 30, 573 2003.
18. Horch, R.E., Bannasch, H., Kopp, J., Andree, C., and Stark, G.B. Single-cell suspensions of cultured human keratinocytes in fibrin-glue reconstitute the epidermis. Cell Trans- plant 7, 309, 1998.
19. Escamez, M.J., Garcia, M., Larcher, F., Meana, A., Munoz, E., Jorcano, J.L., and Del Rio, M. An in vivo model of wound healing in genetically modified skin-humanized mice. J Invest Dermatol 123, 1182, 2004.
20. Wang, J., Ding, J., Jiao, H., Honardoust, D., Momtazi, M., Shankowsky, H.A., and Tredget, E.E. Human hypertrophic scar-like nude mouse model: characterization of the molecular and cellular biology of the scar process. Wound Repair Regen 19, 274, 2011.
21. Hu, K., Dai, Y., Hu, Q., Li, J., Yuan, J., Li, J., and Wu, Q. An experimental study on the repair of full skin loss of nude mice with composite graft of epidermal stem cells. Burns 32, 416, 2006.
22. Masseth, R. Apligraf: a promising new wound care treatment for the 21st century. J Natl Assoc Orthop Technol 8, 22, 2002.
23. Olsen, L., Sherratt, J., and Maini, P. A mechanochemical model for adult dermal wound contraction and the permanence of the contracted tissue displacement profile. J Theor Biol 177, 113, 1995.
24. Tranquillo, R., and Murray, J.D. Mechanistic model of wound contraction. J Surg Res 55, 233, 1993.
25. Stadelmann, W.K., Digenis, A.G., and Tobin, G.R. Physiology and healing dynamics of chronic cutaneous wounds. Am J Surg 176, 26S, 1998.
26. Weber, S.M., Peterson, K.A., Durkee, B., Qi, C., Longino, M., Warner, T., Lee, Jr., F.T., and Weichert, J.P. Imaging of murine liver tumor using microCT with a hepatocyte- selective contrast agent: accuracy is dependent on adequate contrast enhancement. J Surg Res 119, 41, 2004.
27. Diegelmann, R.F., and Evans, M.C. Wound healing: an overview of acute, fibrotic and delayed healing. Front Biosci 9,

283, 2004.

28. Kalyanaraman, B., and Boyce, S.T. Wound healing on athymic mice with engineered skin substitutes fabricated with keratinocytes harvested from an automated bioreactor. J Surg Res 152, 296, 2009.

29. Boyce, S.T., Supp, A.P., Swope, V.B., and Warden, G.D. Vitamin C regulates keratinocyte viability, epidermal bar- rier, and basement membrane in vitro, and reduces wound contraction after grafting of cultured skin substitutes. J Invest Dermatol 118, 565, 2002.

30. Kang, X., Xie, Y., and Kniss, D.A. Adipose tissue model using three-dimensional cultivation of preadipocytes seeded onto fibrous polymer scaffolds. Tissue Eng 11, 458, 2005.

31. Jain, R.K., Au, P., Tam, J., Duda, D.G., and Fukumura, D. Engineering vascularized tissue. Nat Biotechnol 23, 821, 2005.

32. Huss, F.R., and Kratz, G. Adipose tissue processed for lipo injection shows increased cellular survival in vitro when tissue engineering principles are applied. Scand J Plast Reconstr Surg Hand Surg 36, 166, 2002.

33. Kremer, M., Lang, E., and Berger, A.C. Evaluation of dermal-epidermal skin equivalents ('composite-skin') of human keratinocytes in a collagen-glycosaminoglycan matrix(Integra artificial skin). Br J Plast Surg 53, 459, 2000.

34. Kempf, M., Miyamura, Y., Liu, P.Y., Chen, A.C., Nakamura, H., Shimizu, H., Tabata, Y., Kimble, R.M., and McMillan, J.R. A denatured collagen microfiber scaffold seeded with human fibroblasts and keratinocytes for skin grafting. Biomaterials 32, 4782, 2011.